

ORNL/TM-11523



3 4456 0349397 6

OAK RIDGE
NATIONAL
LABORATORY



Formation of Magnetic Islands
Due to Field Perturbations
in Toroidal Stellarator
Configurations

D. K. Lee
J. H. Harris
G. S. Lee

OAK RIDGE NATIONAL LABORATORY
CENTRAL RESEARCH LIBRARY
CIRCULATION SECTION
ASPIN ROOM 175

LIBRARY LOAN COPY
DO NOT TRANSFER TO ANOTHER PERSON

If you wish someone else to see this report, send in name with report and the library will arrange a loan.

OPERATED BY
MARTIN MARIETTA ENERGY SYSTEMS, INC.
FOR THE UNITED STATES
DEPARTMENT OF ENERGY

This report has been reproduced directly from the best available copy.

Available to DOE and DOE contractors from the Office of Scientific and Technical Information, P.O. Box 62, Oak Ridge, TN 37831; prices available from (615) 576-8401, FTS 626-8401.

Available to the public from the National Technical Information Service, U.S. Department of Commerce, 5285 Port Royal Rd., Springfield, VA 22161.

NTIS price codes—Printed Copy: A03 Microfiche A01

This report was prepared as an account of work sponsored by an agency of the United States Government. Neither the United States Government nor any agency thereof, nor any of their employees, makes any warranty, express or implied, or assumes any legal liability or responsibility for the accuracy, completeness, or usefulness of any information, apparatus, product, or process disclosed, or represents that its use would not infringe privately owned rights. Reference herein to any specific commercial product, process, or service by trade name, trademark, manufacturer, or otherwise, does not necessarily constitute or imply its endorsement, recommendation, or favoring by the United States Government or any agency thereof. The views and opinions of authors expressed herein do not necessarily state or reflect those of the United States Government or any agency thereof.

ORNL/TM-11523
Dist. Category UC-426

Fusion Energy Division

**FORMATION OF MAGNETIC ISLANDS DUE TO
FIELD PERTURBATIONS IN TOROIDAL
STELLARATOR CONFIGURATIONS**

**D. K. Lee
J. H. Harris
G. S. Lee**

Date Published: June 1990

Prepared for the
Office of Fusion Energy
Budget Activity No. AT 10

Prepared by the
OAK RIDGE NATIONAL LABORATORY
Oak Ridge, Tennessee 37831-6285
operated by
MARTIN MARIETTA ENERGY SYSTEMS, INC.
for the
U.S. DEPARTMENT OF ENERGY
under contract DE-AC05-84OR21400



3 4456 0349397 6

CONTENTS

ABSTRACT	v
1. INTRODUCTION	1
2. FORMULATION IN MAGNETIC FLUX COORDINATES	4
3. COMPARISON WITH NUMERICAL RESULTS	10
4. SUMMARY	19
ACKNOWLEDGMENT	20
REFERENCES	21

ABSTRACT

An explicit formulation is developed to determine the width of a magnetic island separatrix generated by magnetic field perturbations in a general toroidal stellarator geometry. A conventional method is employed to recast the analysis in a magnetic flux coordinate system without using any simplifying approximations. The island width is seen to be proportional to the square root of the Fourier harmonic of B^ρ/B^ζ that is in resonance with the rational value of the rotational transform, where B^ρ and B^ζ are contravariant normal and toroidal components of the perturbed magnetic field, respectively. The procedure, which is based on a representation of three-dimensional flux surfaces by double Fourier series, allows rapid and fairly accurate calculation of the island widths in real vacuum field configurations, without the need to follow field lines through numerical integration of the field line equations. Numerical results of the island width obtained in the flux coordinate representation for the Advanced Toroidal Facility agree closely with those determined from Poincaré puncture points obtained by following field lines.

1. INTRODUCTION

Toroidal confinement devices having rotational transform are highly sensitive to perturbing magnetic fields that resonate with rational values of the rotational transform ($\epsilon = n/m$). Sources for these perturbation (error) fields include coil misalignments during installation, imperfections in coil windings, fields from bus-works and leads, and the presence of ferromagnetic materials in the vicinity [1, 2]. Recently, the mechanism of magnetic-surface breakup and island formation by magnetic field irregularities has received considerable attention, and significant advances have been reported by many authors [3–13].

In a cylindrically symmetric system of flux surfaces, if the perturbation field contains a component normal to an (unperturbed) rational surface with $\epsilon = n/m$ and the resonant helical harmonic of this component is of the type

$$B_{mn} = b_{mn} \sin(m\theta - n\phi + \gamma), \quad (1)$$

then the maximum width of a magnetic island generated at the resonant surface is given by [9–11]

$$d_0 = 4 \left| \frac{b_{mn} r_0 \epsilon_0}{m \langle B_\theta(r) \rangle \epsilon'_0} \right|^{1/2}, \quad (2)$$

where ϵ is the rotational transform, $\epsilon' = d\epsilon/dr$ is the shear, r is the minor radius, and $\langle B_\theta(r) \rangle$ is the average poloidal component of the magnetic field at the flux surface r . Subscripts “0” in Eq. (2) mean that the quantities are evaluated at the rational surface $r = r_0$ with $\epsilon_0 = n/m$. Somewhat different but fundamentally equivalent forms are given in Refs. [3, 6–8], and an improved formula correct to second order in inverse aspect ratio is derived in Ref. [12].

The result given by Eq. (2) is basically accurate in the approximation of an infinite-aspect-ratio toroidal magnetic field configuration, in which magnetic flux

surfaces are assumed to be concentric circles and hence the toroidal coupling of the Fourier components arising from noncircularity and shift of the flux surfaces is entirely neglected. In one way or another, this type of assumption is usually made in carrying out analytical studies of the effect of field perturbations on the magnetic flux surfaces in toroidal stellarator configurations [3–12]. If, however, a perturbation B_{mn} given by Eq. (1) is applied to an actual toroidal system, islands are produced not only on the surface with $\iota = n/m$ but also on other surfaces with $\iota = n/(m \pm 1)$, $m > 1$, because of mode coupling caused by toroidicity. This means that nonresonant perturbations $B_{m+1,n}$ and $B_{m-1,n}$ also generate islands at the surface with $\iota = n/m$, although these islands are somewhat smaller than those due to B_{mn} with the same magnitude. In the case of the Advanced Toroidal Facility (ATF), island widths at the $\iota = 1/2$ surface due to $B_{1,1}$ and $B_{3,1}$ are both about 48% of the width of the island due to $B_{2,1}$.

For the practical analysis of perturbations to the fixed geometry of an existing stellarator experiment (such as the ATF), it is very useful to break down error fields into their Fourier components and then calculate the island widths at the various rational surfaces without resorting to the tedious “standard” method [2, 14] of following field lines for each of the realistic perturbations under consideration. The Cary-Hanson technique [15–17], which is not directly related to finding island widths, employs Hamiltonian dynamics to estimate the island width by using information obtained from integrating along the closed field line at the island center. This method is computationally far more efficient than the standard method, and the numerical results obtained for the ATF are accurate to at least within 5% for the $\iota = 1/2$ surface and 30% for the $\iota = 2/3$ surface [13]. However, for applications such as experiments in which the configuration is already fixed and there are many possible sources of error fields, it is frequently desirable to analyze the effects of

external perturbations using harmonic analysis and an expression like Eq. (2). For example, when one is trying to find the error fields responsible for islands measured experimentally using electron beams [2], it is useful to study the effects of many possible error sources quickly so as to reduce the number of possibilities that must be investigated in more detail.

The general technique of deriving island width formulas under various types of approximations is well known and can be found in the literature, including Refs. [3–12]. In this report, we employ the same method to develop a quite *general and accurate* numerical procedure for calculating island widths in an arbitrary three-dimensional toroidal geometry, without introducing any approximations. The present study, therefore, differs only in this respect from the majority of the earlier investigations [3–12], which are primarily concerned with analytic derivations under simplifying assumptions, such as zero or small inverse aspect ratio, circular (or nearly circular) and concentric flux surfaces, small helical field, and expansions in terms of certain small parameters. Application of the island width formula to the actual ATF vacuum magnetic geometry shows that numerical results based on the formula and those obtained by following field lines in the standard method agree quite closely even though the involved perturbations are substantial.

2. FORMULATION IN MAGNETIC FLUX COORDINATES

In this section, we present a brief derivation of the expression for the magnetic island width by following basically the same method employed in Refs. [3–12]. Here, however, no special approximations are made; hence, the formulation is quite general and the results are expected to be more accurate than those based on many conventional approximations. The only assumption used is that the toroidal flux surface under consideration is closed and satisfies the stellarator symmetry conditions

$$R(\rho, -\theta, -\zeta) = R(\rho, \theta, \zeta),$$

$$Z(\rho, -\theta, -\zeta) = -Z(\rho, \theta, \zeta),$$

and can be represented by a double Fourier series [18, 19]:

$$R(\rho, \theta, \zeta) = \sum_{m,n} R_{mn}(\rho) \cos(m\theta - n\zeta), \quad (3)$$

$$Z(\rho, \theta, \zeta) = \sum_{m,n} Z_{mn}(\rho) \sin(m\theta - n\zeta), \quad (4)$$

where ζ and θ represent toroidal and poloidal angles, respectively, and ρ is a radial coordinate labeling the toroidal surfaces. Here, we define

$$\rho = \left(\frac{\Phi}{\pi B_0} \right)^{1/2}, \quad (5)$$

where $\Phi = \Phi(\rho)$ is the toroidal magnetic flux enclosed in the magnetic surface ρ and B_0 is the average magnetic field at the axis, $\rho = 0$. As in the inverse representation of MHD equilibria [20], the magnetic flux coordinates (ρ, θ, ζ) are considered the independent variables in Eqs. (3) and (4), and the cylindrical coordinates (R, ϕ, Z) are the dependent variables, with

$$\phi = \zeta. \quad (6)$$

The unperturbed magnetic field \vec{B}_0 can be expressed in a contravariant vector form as [18, 19, 21]

$$\vec{B}_0 = \nabla\Phi \times \nabla\beta, \quad (7)$$

$$\nabla\beta = \nabla\theta^* - \tau(\rho)\nabla\zeta, \quad (8)$$

$$\theta^* = \theta + \lambda(\rho, \theta, \zeta), \quad (9)$$

where $\lambda(\rho, \theta, \zeta)$ is a stream function relating the poloidal angle θ to the magnetic flux coordinate θ^* . In the (ρ, θ^*, ζ) coordinate system, the magnetic field lines are straight on any surface given by $\rho = \text{const}$, since Eqs. (7) and (8) give the local rotational transform

$$\frac{\vec{B}_0 \cdot \nabla\theta^*}{\vec{B}_0 \cdot \nabla\zeta} = \tau(\rho),$$

which is a function of ρ alone. Thus, along the unperturbed field line, we have

$$\frac{d\theta^*}{d\zeta} = \tau(\rho), \quad (10)$$

which is one of two equations used to describe the field line.

To obtain a useful form of the other equation, we write

$$\vec{r} = R\hat{r} + Z\hat{z}, \quad (11)$$

$$d\vec{r} = d\rho\vec{e}_\rho + d\theta\vec{e}_\theta + d\zeta\vec{e}_\zeta, \quad (12)$$

$$\begin{aligned} \vec{B} &= \vec{B}_0 + \delta\vec{B}, \\ &= B_r\hat{r} + B_\phi\hat{\phi} + B_z\hat{z}, \\ &= B^\rho\vec{e}_\rho + B^\theta\vec{e}_\theta + B^\zeta\vec{e}_\zeta, \end{aligned} \quad (13)$$

where $(\hat{r}, \hat{\phi}, \hat{z})$ is the set of orthonormal basis vectors of the (R, ϕ, Z) system, $\delta\vec{B}$ represents the perturbation (error) field, and

$$B^i = \vec{B} \cdot \vec{e}^i \quad (14)$$

are the contravariant components of \vec{B} . In Eqs. (12)–(14),

$$\vec{e}_i = \frac{\partial \vec{r}}{\partial u_i} \quad (15)$$

and

$$\vec{e}^i = \nabla u_i \quad (16)$$

are the covariant and contravariant basis vectors, respectively, and (u_1, u_2, u_3) represent (ρ, θ, ζ) . Since $B_\phi = RB^\zeta$, Eqs. (6), (12), and (13) yield

$$\frac{d\rho}{d\phi} = \frac{RB^\rho}{B_\phi}. \quad (17)$$

Note that $B_0^\rho = 0$, and hence $B^\rho = \vec{B} \cdot \hat{n} |\nabla \rho|$ is due entirely to $\delta \vec{B}$ (\hat{n} is the unit vector normal to the unperturbed flux surface).

In general, the right side of Eq. (17) can be expanded in helical harmonics as

$$\begin{aligned} \frac{RB^\rho}{B_\phi} &= \sum_{m,n} a_{mn}(\rho) \cos(m\theta^* - n\phi) + \sum_{mn} b_{mn}(\rho) \sin(m\theta^* - n\phi) \\ &= \sum_{m,n} c_{mn}(\rho) \sin(m\theta^* - n\phi + \gamma_{mn}), \end{aligned} \quad (18)$$

with $c_{mn}(\rho) > 0$. However, in the process of island formation at a given rational surface, the contribution from nonresonant components is far smaller than that from the resonant one. Therefore, at the surface with $\iota(\rho) = n/m$, Eq. (17) may be approximated by

$$\frac{d\rho}{d\phi} = c_{mn}(\rho) \sin \alpha, \quad (19)$$

where

$$\alpha = m\theta^* - n\phi + \gamma_{mn}. \quad (20)$$

Along the field line, the derivatives of α with respect to ϕ become, with Eq. (10),

$$\frac{d\alpha}{d\phi} = m\iota(\rho) - n, \quad (21)$$

$$\frac{d^2\alpha}{d\phi^2} = m\epsilon'(\rho)\frac{d\rho}{d\phi}. \quad (22)$$

Without loss of generality, Eq. (22) can be written as

$$\frac{d^2\alpha}{d\phi^2} = -A \sin \alpha, \quad (23)$$

where

$$A = |m\epsilon'(\rho)c_{mn}(\rho)| \quad (24)$$

may be approximated as a constant in integrating Eq. (23), if the field line does not deviate far from the unperturbed rational surface with $\epsilon = n/m$. The result can then be written in the form

$$\left(\frac{d\alpha}{d\phi}\right)^2 = 4A \left(k^2 - \sin^2 \frac{\alpha}{2}\right). \quad (25)$$

The maximum width of the magnetic island (separatrix) corresponds to $k^2 = 1$ [9, 22],

$$\frac{d\alpha}{d\phi} = 2\sqrt{A} \cos \frac{\alpha}{2}, \quad (26)$$

and is given by

$$d = \int d\rho = 2 \int_0^\pi \frac{d\rho}{d\phi} \left(\frac{d\alpha}{d\phi}\right)^{-1} d\alpha. \quad (27)$$

With substitutions from Eqs. (19) and (26), Eq. (27) finally becomes

$$d = 4 \left| \frac{c_{mn}(\rho)}{m\epsilon'(\rho)} \right|^{1/2}. \quad (28)$$

Note that Eq. (28) gives the island width in the variable ρ (i.e., $d/2$ is the maximum deviation in ρ). The relationship between ρ and the average minor radius $\langle r \rangle$ is discussed in Section 3. If the normal component of the error field B^ρ is given by Eq. (1) and the straight cylindrical geometry is used by approximating Eqs. (3) and (4), (9), and (18), respectively, by

$$R(\rho, \theta, \phi) \approx R_0 + r \cos \theta, \quad Z(\rho, \theta, \phi) \approx r \sin \theta, \quad (29)$$

$$\theta^*(\rho, \theta, \phi) \approx \theta, \quad (30)$$

$$\frac{R(\rho, \theta, \phi)B^\rho(\rho, \theta, \phi)}{B_\phi(\rho, \theta, \phi)} \approx \frac{r_0 \epsilon(r_0) b_{mn}}{\langle B_\theta(r_0) \rangle} \sin(m\theta - n\phi + \gamma), \quad (31)$$

then Eq. (28) reduces to Eq. (2).

We now turn to a method of evaluating the Fourier components of RB^ρ/B_ϕ :

$$c_{mn}(\rho) = [a_{mn}^2(\rho) + b_{mn}^2(\rho)]^{1/2}, \quad (32)$$

where $a_{mn}(\rho)$ and $b_{mn}(\rho)$ are coefficients of $\cos(m\theta^* - n\phi)$ and $\sin(m\theta^* - n\phi)$, respectively, in the Fourier series given by Eq. (18). The quantities that are needed to calculate $c_{mn}(\rho)$ ($R, \vec{B}, \nabla\rho, \vec{e}^i, \vec{e}_i$, etc.) cannot be expressed readily in (ρ, θ^*, ϕ) coordinates; hence, it is more convenient to use (ρ, θ, ϕ) coordinates. Therefore, we write, except for $m = n = 0$,

$$a_{mn}(\rho) = \frac{1}{2\pi^2} \int_0^{2\pi} \int_0^{2\pi} \frac{RB^\rho}{B_\phi} \cos[m\theta^*(\rho, \theta, \phi) - n\phi] \frac{\partial\theta^*}{\partial\theta} d\theta d\phi, \quad (33)$$

$$b_{mn}(\rho) = \frac{1}{2\pi^2} \int_0^{2\pi} \int_0^{2\pi} \frac{RB^\rho}{B_\phi} \sin[m\theta^*(\rho, \theta, \phi) - n\phi] \frac{\partial\theta^*}{\partial\theta} d\theta d\phi, \quad (34)$$

which indicate that we now need to determine two expressions: (1) $\lambda(\rho, \theta, \phi)$ for $\theta^*(\rho, \theta, \phi)$ and $\partial\theta^*/\partial\theta$ and (2) $\nabla\rho$ for $B^\rho = \vec{B} \cdot \nabla\rho$. The Fourier series of $\lambda(\rho, \theta, \phi)$ is of the form [19]

$$\lambda(\rho, \theta, \phi) = \sum_{m,n} \lambda_{mn}(\rho) \sin(m\theta - n\phi), \quad (35)$$

and a convenient and accurate method of calculating $\lambda_{mn}(\rho)$ is described in Ref. [19].

With Eqs. (11) and (15), and $\partial\hat{r}/\partial\phi = \hat{\phi}$, it is straightforward to obtain

$$\vec{e}_\rho = \frac{\partial R}{\partial\rho} \hat{r} + \frac{\partial Z}{\partial\rho} \hat{z}, \quad (36)$$

$$\vec{e}_\theta = \frac{\partial R}{\partial\theta} \hat{r} + \frac{\partial Z}{\partial\theta} \hat{z}, \quad (37)$$

$$\vec{e}_\phi = \frac{\partial R}{\partial\phi} \hat{r} + R\hat{\phi} + \frac{\partial Z}{\partial\phi} \hat{z}, \quad (38)$$

in terms of which \vec{e}^ρ can be written as

$$\begin{aligned}\vec{e}^\rho &= \vec{e}_\theta \times \vec{e}_\phi / \sqrt{g} \\ &= \frac{1}{\sqrt{g}} \left[-R \frac{\partial Z}{\partial \theta} \hat{r} + \left(\frac{\partial R}{\partial \phi} \frac{\partial Z}{\partial \theta} - \frac{\partial R}{\partial \theta} \frac{\partial Z}{\partial \phi} \right) \hat{\phi} + R \frac{\partial R}{\partial \theta} \hat{z} \right],\end{aligned}\quad (39)$$

where

$$\begin{aligned}\sqrt{g} &= \vec{e}_\rho \times \vec{e}_\theta \cdot \vec{e}_\phi \\ &= R \left(\frac{\partial R}{\partial \theta} \frac{\partial Z}{\partial \rho} - \frac{\partial R}{\partial \rho} \frac{\partial Z}{\partial \theta} \right)\end{aligned}\quad (40)$$

is the Jacobian of the transformation from (R, ϕ, Z) to (ρ, θ, ϕ) . Thus, the expression for B^ρ in (ρ, θ, ϕ) coordinates becomes

$$B^\rho = \frac{1}{\sqrt{g}} \left[-B_r R \frac{\partial Z}{\partial \theta} + B_\phi \left(\frac{\partial R}{\partial \phi} \frac{\partial Z}{\partial \theta} - \frac{\partial R}{\partial \theta} \frac{\partial Z}{\partial \phi} \right) + B_z R \frac{\partial R}{\partial \theta} \right].\quad (41)$$

Expressions for the partial derivatives of R , Z , and λ with respect to the flux coordinates (ρ, θ, ϕ) are obtained from Eqs. (3), (4), and (35), respectively.

3. COMPARISON WITH NUMERICAL RESULTS

In this section, we present numerical results for the magnetic islands obtained at two rational surfaces with $\iota = 1/2$ and $1/3$ in the vacuum magnetic configuration of the ATF. Eight examples are considered so that the island widths evaluated with Eq. (28) can be compared with those measured from Poincaré puncture points. A set of such points forming islands at a given toroidal surface is obtained by following the actual field line that produces the maximum islands (and hence the x-points) after enough transits around the torus. In Table I, examples 1–5 and 6–8 are given for surfaces with $\iota = 1/2$ and $1/3$, respectively; the table lists numerical values for (a) the Fourier component c_{mn} obtained from Eq. (32) with $m = 2, 3$ and $n = 1$, (b) the island width d determined from Eq. (28) with $\iota' = 0.02396 \text{ cm}^{-1}$ ($\iota = 1/2$) and 0.007622 cm^{-1} ($\iota = 1/3$), and (c) the actual (computed) island width $\Delta\rho$, which is the maximum difference in ρ between the outer and inner points of an island at a given θ .

TABLE I. NUMERICAL VALUES OF c_{m1} , d , AND $\Delta\rho$ AT RATIONAL SURFACES WITH $\iota = 1/2$ AND $1/3$ FOR ATF

Example	ι	m	c_{m1} (cm)	d (cm)	$\Delta\rho$ (cm)
1	1/2	2	6.743×10^{-2}	4.744	4.77
2	1/2	2	1.570×10^{-2}	2.290	2.30
3	1/2	2	1.570×10^{-2}	2.290	2.28
4	1/2	2	7.750×10^{-2}	5.087	5.05
5	1/2	2	7.589×10^{-3}	1.592	1.57
6	1/3	3	1.125×10^{-2}	2.806	2.81
7	1/3	3	1.849×10^{-3}	1.138	1.12
8	1/3	3	2.245×10^{-3}	1.253	1.25

Perturbation fields of the form

$$\delta\vec{B} = b \cos(\mu\theta^* - \phi)\hat{n} \quad (42)$$

are used in examples 1, 2, and 3 with $\mu = 2, 1,$ and $3,$ respectively. Here $b = 3.0326 \times 10^{-4} B_0,$ where $B_0 = 0.9893$ T is the average toroidal component of the unperturbed field at the magnetic axis. It must be pointed out here that the perturbation field given by Eq. (42) is not a realistic one in a toroidal geometry. However, it appears to serve a useful purpose in demonstrating that nonresonant components of a field error also contribute to island formation at the rational surfaces. In the numerical process of integrating the field lines (at least 500 turns toroidally) with the error field of Eq. (42), we did not observe any indication of difficulties, such as spiraling of the field lines into the island chain or away from it. The perturbation field of examples 4 and 6 is due to the “initial” buswork (before modification) of the ATF configuration, which involved four large sets of uncompensated current feeds to the helical and vertical field coils [2]. This asymmetry was found to be the main source of rather large islands (~ 6 cm wide at the $\iota = 1/2$ surface, as determined by electron beam measurements), and the buswork was later modified by adding a “compensatory” buswork consisting of eight similar loops to produce the 12-fold symmetry. The perturbation field of examples 5 and 7 is due to this “modified” buswork [2]. (In the experiment, this change reduced the island width to ≈ 1 cm at the $\iota = 1/2$ surface.) Example 8 involves an error field resulting from a horizontal linear displacement of the entire upper outer vertical-field coil set by 5 mm. Poincaré puncture plots of Z vs R and ρ vs θ for example 2 are shown in Figs. 1(a) and 1(b), respectively. Similar plots for the other examples are not shown, since they do not look much different except in width.

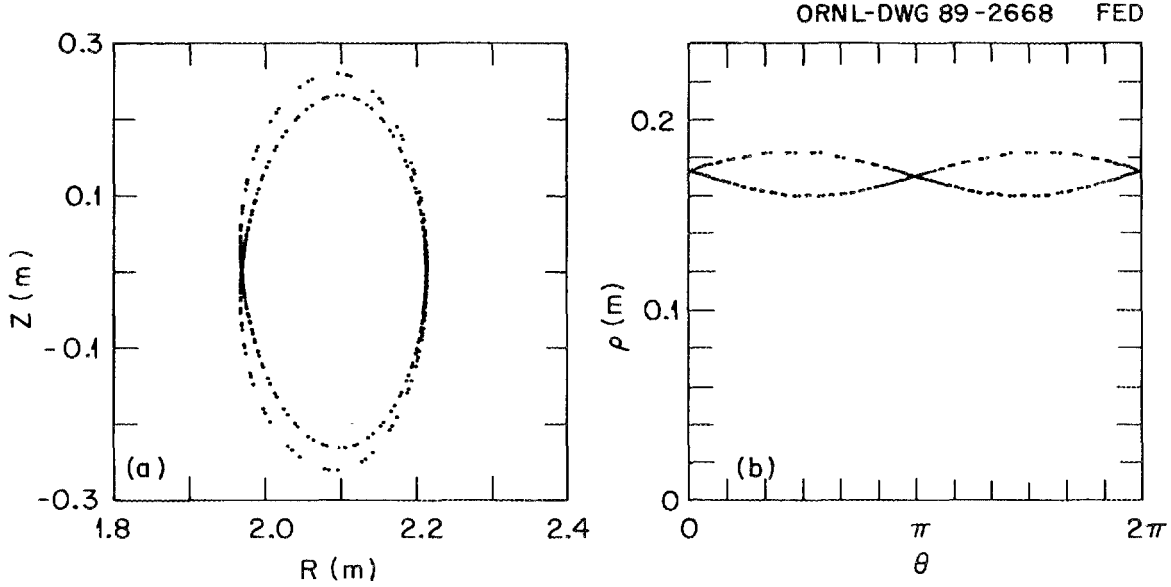


Fig. 1. Poincaré puncture plots of example 2; (a) R vs Z and (b) ρ vs θ .

In general, the validity of Eq. (28) is restricted to the case where only a single perturbation field is taken into account. However, as long as the involved perturbations are not excessively large, a fairly accurate estimation can be made from Eq. (28) even if the error field consists of many overlapping perturbations. Suppose the error field space of a given magnetic configuration is an N -dimensional vector space spanned by basis vectors $\delta\vec{B}_1, \delta\vec{B}_2, \dots, \delta\vec{B}_N$, each representing a small elementary perturbation field. The assumption of “small” perturbations is made here so that the Fourier harmonics $a_{mn}^{(i)}(\rho)$ and $b_{mn}^{(i)}(\rho)$ due to $\delta\vec{B}_i$ can be obtained with the approximation $B_\phi = \vec{B}_0 \cdot \hat{\phi}$ in Eqs. (18), (33), and (34) for $i = 1, 2, \dots, N$. Then, an arbitrary (small) error field can be written as

$$\delta\vec{B} = \sum_{i=1}^N \eta_i \delta\vec{B}_i, \quad (43)$$

and the island width can be determined from Eq. (28) with $c_{mn}(\rho)$ given by

$$c_{mn}(\rho) = \left[\left(\sum_{i=1}^N \eta_i a_{mn}^{(i)}(\rho) \right)^2 + \left(\sum_{i=1}^N \eta_i b_{mn}^{(i)}(\rho) \right)^2 \right]^{1/2}. \quad (44)$$

As an application of Eq. (44), let us consider the ATF configuration with the “modified” buswork, which is the “initial” buswork plus the “compensatory” buswork. Table II lists numerical values of resonant harmonics $a_{mn}(\rho)$, $b_{mn}(\rho)$, and $c_{mn}(\rho)$ obtained for four cases at two surfaces with $\epsilon = 1/2$ and $1/3$. In the table, perturbations involved in cases I, II, and III are the error fields due to the initial, compensatory, and modified buswork, respectively, and in all three cases B_ϕ is approximated by $\vec{B}_0 \cdot \hat{\phi}$ in Eqs. (18), (33), and (34). Case IV is the same as Case III except that the exact form $(\vec{B}_0 + \delta\vec{B}) \cdot \hat{\phi}$ is used for B_ϕ . In all cases, $c_{mn}(\rho)$ is given by

$$c_{mn}(\rho) = [a_{mn}^2(\rho) + b_{mn}^2(\rho)]^{1/2}. \quad (45)$$

Two observations can be made from the results in Table II: (1) values of $a_{mn}(\rho)$ and $b_{mn}(\rho)$ for case III are equal to algebraic sums of the corresponding values from cases I and II, and hence the validity of Eq. (44) is numerically demonstrated, and (2) the very small differences between the numerical values in cases III and IV

TABLE II. NUMERICAL VALUES OF RESONANT HARMONICS a_{mn} , b_{mn} , AND c_{mn} (in units of 10^{-3} cm) AT RATIONAL SURFACES WITH $\epsilon = 1/2$ AND $1/3$

Case	$\epsilon = 1/2$			$\epsilon = 1/3$		
	a_{21}	b_{21}	c_{21}	a_{31}	b_{31}	c_{31}
I	73.627	24.322	77.540	8.6273	7.3092	11.3073
II	-67.199	-20.283	70.193	-6.9730	-6.4670	9.5105
III	6.428	4.039	7.592	1.6543	0.8422	1.8564
IV	6.426	4.036	7.589	1.6540	0.8422	1.8560

suggest that Eq. (44) can be used to determine $c_{mn}(\rho)$ quite accurately when two or more overlapping perturbations are present (if their magnitudes are not very large).

Next we turn to a close examination of mode couplings that contribute to the resonant harmonic amplitude $c_{mn}(\rho)$ appearing in Eq. (28). The source function of $c_{mn}(\rho)$ is the product of four terms — R , $|\nabla\rho|$, $1/B_\phi$, and $\delta\vec{B} \cdot \hat{n}$. To see how and how much various modes of each of these terms contribute, we consider the case of example 4: $\delta\vec{B}$ from the “initial” buswork and the flux surface with $\tau = 1/2$. The stellarator symmetry given by Eqs. (1) and (2) and the 12-fold symmetry of the unperturbed field imply that all the sine components of R and $|\nabla\rho|$ vanish and the cosine components have modes of the form $(m, \pm 12\nu)$, where m and ν are non-negative integers; such modes are designated (m_0, n_0) . Since B_ϕ is the perturbed field, the components missing in the series of R and $|\nabla\rho|$ do not necessarily vanish in the series of $1/B_\phi$ and $R|\nabla\rho|/B_\phi$, but their magnitudes are too small to merit further consideration here. Table IIIa lists (m_0, n_0) modes and coefficients of $\cos(m_0\theta^* - n_0\phi)$ in Fourier series of R , $1/B_\phi$, $|\nabla\rho|$, and $R|\nabla\rho|/B_\phi$, which make dominant contributions to the resonant harmonic $c_{21}(\rho)$. Modes that give amplitudes of $R|\nabla\rho|/B_\phi$ that are less than 0.01 m/T are not shown. While only a single group of modes is dominant in the series of $R|\nabla\rho|/B_\phi$, the mode spectrum of $B_n = B^\rho/|\nabla\rho| = \delta\vec{B} \cdot \hat{n}$ is quite broad, and there are no particular dominant groups. It suffices to consider only the modes of B_n that couple with (m_0, n_0) of $R|\nabla\rho|/B_\phi$ to yield a (2,1) mode for RB^ρ/B_ϕ . We call such modes (m_1, n_1) : $(m_0 + m_1, n_0 + n_1) = \pm(2, 1)$ or $(m_0 - m_1, n_0 - n_1) = \pm(2, 1)$. In Table IIIb the (m_1, n_1) modes and coefficients of $\cos(m\theta^* - n\phi)$ and $\sin(m\theta^* - n\phi)$ for the Fourier series of B_n are listed. Net results of couplings between the (m_0, n_0) and (m_1, n_1) modes given in Tables IIIa and IIIb, respectively, are shown in Table IIIc, where resonant harmonics a_{21} , b_{21} , and c_{21} of RB^ρ/B_ϕ are listed (in units of 10^{-2} cm) for each (m_0, n_0) mode separately. The table clearly shows that the (1,0) mode

TABLE IIIa. COEFFICIENTS OF $\cos(m_0\theta^* - n_0\phi)$ IN FOURIER SERIES OF R , $1/B_\phi$, $\|\nabla\rho\|$, AND $R\|\nabla\rho\|/B_\phi$ FOR THE CONFIGURATION OF EXAMPLE 4

(m_0, n_0)	R (m)	$\frac{1}{B_\phi} \left(\frac{1}{\text{T}}\right)$	$ \nabla\rho $	$\frac{R \nabla\rho }{B_\phi} \left(\frac{\text{m}}{\text{T}}\right)$
(0,0)	2.0651	1.0226	1.0473	2.2476
(1,0)	0.1481	0.0949	0.3269	1.0469
(2,0)	0.0344	0.0097	0.1045	0.3355
(3,0)	0.0042	-0.0036	0.0181	0.0675
(4,0)	-0.0003	-0.0013	-0.0112	-0.0185
(5,0)	-0.0002	0.0003	-0.0109	-0.0249
(6,0)	0.0000	0.0004	-0.0043	-0.0114
(0,12)	-0.0001	-0.0251	0.0274	0.0963
(1,12)	-0.0306	0.0021	-0.0105	-0.0458
(1,-12)	0.0037	-0.0036	-0.0043	0.0108
(2,12)	-0.0104	0.0887	0.2199	0.2732
(3,12)	-0.0025	0.0466	0.1996	0.3258
(4,12)	-0.0003	0.0119	0.0730	0.1379
(6,12)	0.0000	-0.0008	-0.0099	-0.0199

of $R|\nabla\rho|/B_\phi$ gives the most dominant toroidal effect. At this point it must be remarked that examples 1-3 in Table I are special cases of coupling in which only a single cosine component of B_n is present; thus, the numerical results of c_{21} for these three examples can easily be determined from the values of b in Eq. (42) and the (0,0) and (1,0) coefficients of $R|\nabla\rho|/B_\phi$ listed in Table IIIa.

We conclude this section with a few remarks concerning numerical procedures and results.

1. Let us define the average minor radius of the flux surface with label ρ by

$$\langle r \rangle = \frac{1}{N\pi} \sum_{n=1}^N [A(\rho, \phi_n)]^{1/2}, \quad (46)$$

where $A(\rho, \phi)$ is the cross-sectional area of the flux surface at the toroidal angle ϕ , and $\phi_n = 2n\pi/N$, $n = 1, 2, \dots, N$. Our numerical results for ρ and $\langle r \rangle$

TABLE IIIb. COEFFICIENTS OF $\cos(m_0\theta^* - n_0\phi)$
 $\sin(m_1\theta^* - n_1\phi)$ IN FOURIER SERIES OF
 $\delta\vec{B} \cdot \hat{n}$ FOR THE CONFIGURATION OF
EXAMPLE 4. THE LISTED MODES (m_1, n_1)
CONTRIBUTE TO ISLAND FORMATION BY
COUPLING WITH (m_0, n_0) MODES GIVEN
IN TABLE IIIa.

(m_1, n_1)	Cosine coefficient (G)	Sine coefficient (G)
(2,1)	-2.2945	-0.9715
(1,1)	-2.8430	0.9624
(3,1)	-1.0189	-0.9869
(0,1)	0.2045	-1.4479
(4,1)	-0.2942	-0.4680
(1,-1)	1.7796	5.3134
(5,1)	-0.0553	-0.1183
(2,-1)	2.2488	-2.7710
(6,1)	-0.0197	-0.0077
(3,-1)	1.2957	-0.8105
(7,1)	-0.0196	0.0004
(2,-11)	-0.9185	-0.7869
(2,13)	0.2513	0.2276
(1,-11)	-1.0698	-0.6391
(3,13)	0.1720	-0.1537
(0,11)	-0.0525	-0.0256
(4,13)	0.3068	-0.0415
(1,11)	-1.3311	0.6503
(5,13)	0.2546	0.1086
(2,11)	-0.5042	-0.5193
(6,13)	0.0953	0.1087

obtained with $N = 192$ for the ATF reveal that the values of ρ and $\langle r \rangle$ differ by less than 0.2% in the regions near surfaces with $\epsilon = 1/2$ and $1/3$. For practical purposes, therefore, the island width given by Eq. (28) may be viewed as the average value of the local maximum island width seen in the R - Z plane as in Fig. 1(a). Note that the island width is a function of ϕ and for a given toroidal

TABLE IIIc. INDIVIDUAL RESONANT HARMONICS a_{21} , b_{21} , AND c_{21} (10^{-2} cm) FOR RB^{ρ}/B_{ϕ} , WHICH RESULT FROM COUPLING OF MODES (m_0, n_0) AND (m_1, n_1) LISTED IN TABLES IIIa AND IIIb, RESPECTIVELY

(m_0, n_0)	(m_1, n_1)	a_{21}	b_{21}	c_{21}
(0,0)	(2,1)	-5.1571	-2.1836	5.6004
(1,0)	(1,1), (3,1)	-2.0215	-0.0128	2.0216
(2,0)	(0,1), (4,1)	-0.0151	-0.3214	0.3217
(3,0)	(1,-1), (5,1)	0.0582	-0.1834	0.1924
(4,0)	(2,-1), (6,1)	-0.0207	-0.0256	0.0329
(5,0)	(3,-1), (7,1)	-0.0159	-0.0101	0.0188
(0,12)	(2,-11), (2,13)	-0.0321	-0.0269	0.0419
(1,12)	(1,-11), (3,13)	0.0206	0.0182	0.0274
(2,12)	(0,11), (4,13)	0.0347	-0.0022	0.0348
(3,12)	(1,11), (5,13)	-0.1754	-0.0882	0.1963
(4,12)	(2,11), (6,13)	-0.0282	0.0433	0.0517
Total (Example 4)		-7.3609	-2.4262	7.7504

plane there are m islands (with generally different widths) at the $\tau = n/m$ rational surface.

2. In examples 1-8, the number of modes whose Fourier amplitudes are larger than the resonant amplitude c_{mn} (listed in Table I) are 1, 12, 12, 7, 79, 39, 67, and 14, respectively. The close numerical agreement between d and $\Delta\rho$ demonstrated in Table I verifies the assumption that the resonant component in Eq. (19) plays the dominant role in the island formation.
3. The initial buswork involved 12 loops with a total of 84 straight wire segments, and the modified buswork has 32 loops with a total of 259 segments; thus, the perturbations used in examples 4-7 are quite complex and not small. Nevertheless, the accuracy of Eq. (28) is better than 2% in these cases, and errors in other examples are only about 0.5% or less.

4. Determination of d from Eq. (28) requires evaluation of $R_{mn}(\rho)$ and $Z_{mn}(\rho)$ not only at the rational surface but also at many adjacent surfaces, since calculation of \sqrt{g} [needed for B^ρ and $\lambda(\rho, \theta, \phi)$] involves $\partial R_{mn}/\partial\rho$ and $\partial Z_{mn}/\partial\rho$, which must be obtained numerically [19].
5. The method described in this paper is self-consistent only for vacuum magnetic fields and not for finite-beta equilibria.

4. SUMMARY

We used a known method of Fourier analysis in the magnetic flux coordinate system to develop a formulation suitable for accurate numerical evaluation of island widths due to magnetic irregularities in vacuum field configurations of actual toroidal systems. Application of the width formula to the ATF configuration yields results which differ by less than 2% from those determined in the standard method by following field lines through numerical integration of the field line equations. The calculations also demonstrate the importance of toroidal mode coupling by showing that considerable contributions are made at the rational surface with $\iota = n/m$ by nonresonant field error harmonics $B_{m+1,n}$ and $B_{m-1,n}$. The method studied in this paper is useful in analyzing the effects of various field perturbations in a *fixed* magnetic configuration.

ACKNOWLEDGMENT

The authors are grateful to S. P. Hirshman, J. R. Cary, and J. D. Hanson for many useful comments and suggestions.

REFERENCES

1. CARRERAS, B. A., GRIEGER, G., HARRIS, J. H., et al., Nucl. Fusion **28** (1988) 1613.
2. HARRIS, J. H., JERNIGAN, T. C., BENSON, R. D., et al., Fusion Technol. **17** (1990) 51.
3. KOVRIZHNYKH, L. M., Zh. Tekh. Fiz. **31** (1961) 888; **32** (1962) 526.
4. MOROZOV, A. I., SOLOV'EV, L. S., Zh. Eksp. Teor. Fiz. **45** (1963) 955.
5. SOLOV'EV, L. S., SHAFRANOV, V. D., in Reviews of Plasma Physics, Vol. 5, Chap. 1 (LEONTOVICH, M. A., Ed.), Consultants Bureau, New York (1970).
6. ROSENBLUTH, M. N., SAGDEEV, R. Z., TAYLOR, J. B., ZASLAVSKY, G. M., Nucl. Fusion **6** (1966) 297.
7. FILONENKO, N. N., SAGDEEV, R. Z., ZASLAVSKY, G. M., Nucl. Fusion **7** (1967) 253.
8. DANILKIN, I. S., in Proc. P. N. Lebedev Phys. Inst. Acad. Sci. USSR **65** (1973) (in Russian). [English translation: Consultants Bureau, New York (1974) 23.]
9. MATSUDA, S., YOSHIKAWA, M., Jpn. J. Appl. Phys. **14** (1975) 87.
10. RECHESTER, A. B., STIX, T. H., Phys. Rev. Lett. **36** (1976) 587.
11. REIMAN, A. H., BOOZER, A. H., Phys. Fluids **27** (1984) 2446.
12. ZHENG, S. B., WOOTTON, A. J., Magnetic Island Widths in Tokamaks, FRCR-294, University of Texas, Austin (1987).
13. CARY, J. R., HANSON, J. D., CARRERAS, B. A., LYNCH, V. E., Simple method for calculating island widths, in Proc. 7th Int. Stellarator Workshop (Oak Ridge, 1989), IAEA, Vienna (in press).

14. LYON, J. F., CARRERAS, B. A., CHIPLEY, K. K., et al., Fusion Technol. **10** (1986) 179.
15. CARY, J. R., Phys. Fluids **27** (1984) 119.
16. HANSON, J. D., CARY, J. R., Phys. Fluids **27** (1984) 767.
17. CARY, J. R., HANSON, J. D., Phys. Fluids **29** (1986) 2464.
18. HIRSHMAN, S. P., WHITSON, J. C., Phys. Fluids **26** (1983) 3553.
19. LEE, D. K., HARRIS, J. H., HIRSHMAN, S. P., NEILSON, G. H., Nucl. Fusion **28** (1988) 1351.
20. BAUER, F., BETACOURT, O., GARABEDIAN, P., A Computational Method in Plasma Physics, Springer-Verlag, New York (1978) Chap. 2.
21. KRUSKAL, M. D., KULSRUD, R. M., Phys. Fluids **1** (1958) 265.
22. HAYASHI, C., Nonlinear Oscillation in Physical Systems, McGraw-Hill, New York (1964).

INTERNAL DISTRIBUTION

- | | |
|--------------------|---|
| 1-5. D. K. Lee | 22. V. E. Lynch |
| 6-10. J. H. Harris | 23. M. J. Saltmarsh |
| 12. C. C. Baker | 24. J. Sheffield |
| 13. L. A. Berry | 25-26. Laboratory Records Department |
| 14. B. A. Carreras | 27. Laboratory Records, ORNL-RC |
| 15. L. A. Charlton | 28-29. Central Research Library |
| 16. R. J. Colchin | 30. Document Reference Section |
| 17. N. Dominguez | 31. Fusion Energy Division Library |
| 18. R. A. Dory | 32-33. Engineering Technology/Fusion
Energy Division Publications Office |
| 19. J. L. Dunlap | 34. ORNL Patent Office |
| 20. H. H. Haselton | |
| 21. M. S. Lubell | |

EXTERNAL DISTRIBUTION

35. G. S. Lee, Plasma Fusion Center, Massachusetts Institute of Technology, Cambridge, MA 02139
36. Office of the Assistant Manager for Energy Research and Development, U.S. Department of Energy, Oak Ridge Operations Office, P.O. Box E, Oak Ridge, TN 37831
37. J. D. Callen, Department of Nuclear Engineering, University of Wisconsin, Madison, WI 53706-1687
38. R. W. Conn, Department of Chemical, Nuclear, and Thermal Engineering, University of California, Los Angeles, CA 90024
39. N. A. Davies, Acting Director, Office of Fusion Energy, Office of Energy Research, ER-50 Germantown, U.S. Department of Energy, Washington, DC 20545
40. S. O. Dean, Fusion Power Associates, Inc., 2 Professional Drive, Suite 248, Gaithersburg, MD 20879
41. H. K. Forsen, Bechtel Group, Inc., Research Engineering, P.O. Box 3965, San Francisco, CA 94119
42. J. R. Gilleland, L-644, Lawrence Livermore National Laboratory, P.O. Box 5511, Livermore, CA 94550
43. R. W. Gould, Department of Applied Physics, California Institute of Technology, Pasadena, CA 91125
44. R. A. Gross, Plasma Research Laboratory, Columbia University, New York, NY 10027
45. D. M. Meade, Princeton Plasma Physics Laboratory, P.O. Box 451, Princeton, NJ 08543
46. M. Roberts, International Programs, Office of Fusion Energy, Office of Energy Research, ER-52 Germantown, U.S. Department of Energy, Washington, DC 20545
47. W. M. Stacey, School of Nuclear Engineering and Health Physics, Georgia Institute of Technology, Atlanta, GA 30332

48. D. Steiner, Nuclear Engineering Department, NES Building, Tibbetts Avenue, Rensselaer Polytechnic Institute, Troy, NY 12181
49. R. Varma, Physical Research Laboratory, Navrangpura, Ahmedabad 380009, India
50. Bibliothek, Max-Planck Institut für Plasmaphysik, Boltzmannstrasse 2, D-8046 Garching, Federal Republic of Germany
51. Bibliothek, Institut für Plasmaphysik, KFA Jülich GmbH, Postfach 1913, D-5170 Jülich, Federal Republic of Germany
52. Bibliothek, KfK Karlsruhe GmbH, Postfach 3640, D-7500 Karlsruhe 1, Federal Republic of Germany
53. Bibliotheque, Centre de Recherches en Physique des Plasmas, Ecole Polytechnique Fédérale de Lausanne, 21 Avenue des Bains, CH-1007 Lausanne, Switzerland
54. R. Aymar, CEN/Cadarache, Departement de Recherches sur la Fusion Contrôlée, F-13108 Saint-Paul-lez-Durance Cedex, France
55. Bibliothque, CEN/Cadarache, F-13108 Saint-Paul-lez-Durance Cedex, France
56. Library, Culham Laboratory, UKAEA, Abingdon, Oxfordshire, OX14 3DB, England
57. Library, JET Joint Undertaking, Abingdon, Oxfordshire OX14 3EA, England
58. Library, FOM-Instituut voor Plasmafysica, Rijnhuizen, Edisonbaan 14, 3439 MN Nieuwegein, The Netherlands
59. Library, National Institute for Fusion Science, Chikusa-ku, Nagoya 464-01, Japan
60. Library, International Centre for Theoretical Physics, P.O.Box 586, I-34100 Trieste, Italy
61. Library, Centro Ricerca Energia Frascati, C.P. 65, I-00044 Frascati (Roma), Italy
62. Library, Plasma Physics Laboratory, Kyoto University, Gokasho, Uji, Kyoto 611, Japan
63. Plasma Research Laboratory, Australian National University, P. O. Box 4, Canberra, A.C.T. 2601, Australia
64. Library, Japan Atomic Energy Research Institute, Naka Fusion Research Establishment, 801-1 Mukoyama, Naka-machi, Naka-gun, Ibaraki-ken, Japan
65. G. A. Eliseev, I. V. Kurchatov Institute of Atomic Energy, P. O. Box 3402, 123182 Moscow, U.S.S.R.
66. V. A. Glukhikh, Scientific-Research Institute of Electro-Physical Apparatus, 188631 Leningrad, U.S.S.R.
67. I. Shpigel, Institute of General Physics, U.S.S.R. Academy of Sciences, Ulitsa Vavilova 38, Moscow, U.S.S.R.
68. D. D. Ryutov, Institute of Nuclear Physics, Siberian Branch of the Academy of Sciences of the U.S.S.R., Sovetskaya St. 5, 630090 Novosibirsk, U.S.S.R.
69. O. Pavlichenko, Kharkov Physical-Technical Institute, Academical St. 1, 310108 Kharkov, U.S.S.R.
70. Deputy Director, Southwestern Institute of Physics, P.O. Box 15, Leshan, Sichuan, China (PRC)
71. Director, The Institute of Plasma Physics, P.O. Box 26, Hefei, Anhui, China (PRC)

72. R. A. Blanken, Experimental Plasma Physics Research Branch, Division of Applied Plasma Physics, Office of Energy Research, ER-542, Germantown, U.S. Department of Energy, Washington, DC 20545
73. D. H. Crandall, Division of Applied Plasma Physics, Office of Energy Research, ER-542, Germantown, U.S. Department of Energy, Washington, DC 20545
74. D. Markevich, Division of Applied Plasma Physics, Office of Energy Research, ER-55, Germantown, U.S. Department of Energy, Washington, DC 20545
75. R. H. McKnight, Experimental Plasma Physics Research Branch, Division of Applied Plasma Physics, Office of Energy Research, ER-542, Germantown, U.S. Department of Energy, Washington, DC 20545
76. E. Oktay, Division of Confinement Systems, Office of Energy Research, ER-55, Germantown, U.S. Department of Energy, Washington, DC 20545
77. W. L. Sadowski, Fusion Theory and Computer Services Branch, Division of Applied Plasma Physics, Office of Energy Research, ER-541, Germantown, U.S. Department of Energy, Washington, DC 20545
78. J. W. Willis, Division of Confinement Systems, Office of Energy Research, ER-55, Germantown, U.S. Department of Energy, Washington, DC 205
79. E. Anabitarte, Avenida de los Castros s/n, Dept. de Fisica Aplicada, Universidad de Cantabria, 39005 Santander, Spain
80. F. S. B. Anderson, Torsatron/Stellarator Laboratory, University of Wisconsin, Madison, WI 53706
81. R. A. E. Bolton, IREQ Hydro-Quebec Research Institute, 1800 Monte-St.-Julie, Varennes, P.Q. JOL 2P0, Canada
82. R. L. Freeman, General Atomics, P. O. Box 85608, San Diego, CA 92138-5608
83. R. F. Gandy, Physics Department, Auburn University, Auburn, AL 36849-3511
84. K. W. Gentle, RLM 11.222, Institute for Fusion Studies, University of Texas, Austin, TX 78712
85. R. J. Goldston, Princeton Plasma Physics Laboratory, P.O. Box 451, Princeton, NJ 08543
86. J. C. Hosea, Princeton Plasma Physics Laboratory, P.O. Box 451, Princeton, NJ 08543
87. R. R. Parker, Plasma Fusion Center, NW 16-288, Massachusetts Institute of Technology, Cambridge, MA 02139
88. A. Perez Navarro, Division de Fusion, CIEMAT, Avenida Complutense 22, E-28040 Madrid, Spain
89. Laboratory for Plasma and Fusion Studies, Department of Nuclear Engineering, Seoul National University, Shinrim-dong, Gwanak-ku, Seoul 151, Korea
90. J. L. Johnson, Plasma Physics Laboratory, Princeton University, P.O. Box 451, Princeton, NJ 08543
91. L. M. Kovrizhnykh, Institute of General Physics, U.S.S.R. Academy of Sciences, Ulitsa Vavilova 38, 117924 Moscow, U.S.S.R.
92. O. Motojima, National Institute for Fusion Science, Chikusa-ku, Nagoya 464-01, Japan
93. S. Okamura, Institute of Plasma Physics, Nagoya University, Chikusa-ku, Nagoya 464, Japan
94. V. D. Shafranov, I. V. Kurchatov Institute of Atomic Energy, P.O. Box 3402, 123182 Moscow, U.S.S.R.
95. J. L. Shohet, Torsatron/Stellarator Laboratory, University of Wisconsin, Madison, WI 53706

95. J. L. Shohet, Torsatron/Stellarator Laboratory, University of Wisconsin, Madison, WI 53706
96. H. Wobig, Max-Planck Institut für Plasmaphysik, D-8046 Garching, Federal Republic of Germany
97. F. W. Perkins, Princeton Plasma Physics Laboratory, P.O. Box 451, Princeton, NJ 08543
98. T. Obiki, Plasma Physics Laboratory, Kyoto University, Gokasho, Uji, Kyoto, Japan
99. A. Iiyoshi, National Institute for Fusion Studies, Chikusa-ku, Nagoya 464-01, Japan
100. R. E. Mickens, Atlanta University, Department of Physics, Atlanta, GA 30314
101. M. N. Rosenbluth, University of San Diego, La Jolla, CA 92037
102. D. Schnack, SAIC, 10260 Campus Point Drive, San Diego, CA 92121
103. Duk-In Choi, Department of Physics, Korea Advanced Institute of Science and Technology, P.O. Box 150, Chong Ryang-Ri, Seoul, Korea
104. Library of Physics Department, University of Ioannina, Ioannina, Greece
105. C. De Palo, Library, Associazione EURATOM-ENEA sulla Fusione, CP 65, I-00044 Frascati (Roma), Italy
106. Theory Department Read File, c/o D. W. Ross, Institute for Fusion Studies, University of Texas, Austin, TX 78712
107. Theory Department Read File, c/o R. Parker, Director, Plasma Fusion Center, NW 16-202, Massachusetts Institute of Technology, Cambridge, MA 02139
108. Theory Department Read File, c/o R. White, Princeton Plasma Physics Laboratory, P.O. Box 451, Princeton, NJ 08543
109. Theory Department Read File, c/o L. Kovrizhnykh, Lebedev Institute of Physics, Academy of Sciences, 53 Leninsky Prospect, 117924 Moscow, U.S.S.R.
110. Theory Department Read File, c/o B. B. Kadomtsev, I. V. Kurchatov Institute of Atomic Energy, P.O. Box 3402, 123182 Moscow, U.S.S.R.
111. Theory Department Read File, c/o T. Kamimura, National Institute for Fusion Studies, Nagoya 464, Japan
112. Theory Department Read File, c/o C. Mercier, Departemente de Recherches sur la Fusion Controlee, B.P. No. 6, F-92260 Fontenay-aux-Roses (Seine), France
113. Theory Department Read File, c/o T. E. Stringer, JET Joint Undertaking, Abingdon, Oxfordshire OX14 3EA, United Kingdom
114. Theory Department Read File, c/o R. Briscoe, Culham Laboratory, Abingdon, Oxfordshire OX14 3DB, United Kingdom
115. Theory Department Read File, c/o D. Biskamp, Max-Planck-Institut für Plasmaphysik, Boltzmannstrasse 2, D-8046 Garching, Federal Republic of Germany
116. Theory Department Read File, c/o T. Takeda, Japan Atomic Energy Research Institute, Tokai Fusion Research Establishment, Tokai-mura, Naka-gun, Ibaraki-ken, Japan
117. Theory Department Read File, c/o J. Greene, General Atomics, P.O. Box 85608, San Diego, CA 92138-5608
118. Theory Department Read File, c/o R. Cohen, Lawrence Livermore National Laboratory, P.O. Box 5511, Livermore, CA 94550
119. Theory Department Read File, c/o R. Gerwin, CTR Division, Los Alamos National Laboratory, P.O. Box 1663, Los Alamos, NM 87545

120-172. Given distribution as shown in OSTI-4500, Magnetic Fusion Energy (Category Distribution UC-426, Experimental Plasma Physics)